Time calibration for the end cap TOF system of BESIII[*]

ZHAO Chuan(赵川)[1,2;1)]   SUN Sheng-Sen(孙胜森)[2;2)]   LI Cheng(李澄)[1]

ZHANG Xiao-Jie(张晓杰)[2]   HE Kang-Lin(何康林)[2]   AN Qi(安琪)[1]   CHEN Hong-Fang(陈宏芳)[1]

DAI Hong-Liang(代洪亮)[2]   FENG Chang-Qing(封常青)[1]   HENG Yue-Kun(衡月昆)[2]

HUANG Ya-Qi(黄亚齐)[1]   HUANG Yan-Ping(黄燕萍)[1]   GUO Jian-Hua(郭建华)[1]

LI Wei-Dong(李卫东)[1]   LI Xiu-Rong(李秀荣)[1]   LIU Fang(刘芳)[2]

LIU Huai-Min(刘怀民)[2]   LIU Shu-Bin(刘树彬)[1]   LIU Shu-Dong(刘曙东)[2]

LIU Yong(刘勇)[2]   MA Xiang(马想)[2]   MAO Ze-Pu(毛泽普)[2]

SHAO Ming(邵明)[1]   SUN Yong-Jie(孙勇杰)[1]   SUN Zhi-Jia(孙志嘉)[2]

WU Jin-Jie(吴金杰)[2]   YANG Gui-An(杨桂安)[2]   ZHAO Lei(赵雷)[1]

ZHU Xing-Wang(朱兴旺)[2]   ZUO Jia-Xu(左嘉旭)[2]

[1] Department of Modern Physics, University of Science and Technology of China, Hefei 230026, China
[2] Institute of High Energy Physics, Chinese Academy of Sciences, Beijing 100049, China

Abstract: The time calibration for end cap TOF system of BESIII is studied in this paper. It has achieved about 110 ps time resolution for muons in dimu events. The pulse height correction using electronic scan curve and the predicted time calculated using Kalman filter method are introduced. This paper also describes the study of using electrons and muons as calibration samples.

Key words: time-of-flight detector, offline calibration, time resolution

PACS: 29.40.Mc, 29.85.Fj   **DOI:** 10.1088/1674-1137/35/1/015

1   Introduction

The upgraded Beijing Electron-Positron Collider BEPCII [1] is a double-ring, multi-bunch collider with a designed luminosity of 1×10^{33} cm$^{-2}\cdot$s^{-1} at 1.89 GeV, an improvement of a factor of 100 times with respect to the BEPC. The Beijing Spectrometer (BESIII) [2, 3], which will operate at BEPCII, is a high precision general purpose detector which is designed for the high luminosity in the τ-charm energy region. Particle identification (PID) plays an essential role in the experimental study of τ-charm physics. The time-of-flight (TOF) detector systems based on plastic scintillation counters have been very powerful tools for particle identification in collider detectors. Its capability of PID is determined by the flight time difference of particles of different species and the time resolution of the detector. This paper describes the

scheme of time calibration for the end cap TOF using various physics data acquired on BESIII.

2   TOF system in the BESIII detector

The BESIII detector consists of a beryllium beam pipe, a helium-based small-cell multilayer drift chamber (MDC), a time-of-flight (TOF) system, a CsI(Tl) crystal calorimeter (EMC), a superconducting solenoidal magnet with a field of 1 T, and a muon identifier (MU) of resistive plate counters (RPC) interleaved with the magnet yoke plates. The physics program of the BESIII experiment covers charmonium physics, D-physics, spectroscopy of light hadrons, τ-physics and the search for new physics, etc.

The cross-sectional view of the TOF system inside the CsI crystal calorimeter is shown in Fig. 1.

The time-of-flight system is based on plastic scintillator bars read out by fine mesh photomultiplier tubes (PMTs). It consists of a barrel and two end caps. The barrel TOF consists of two layers of 88 plastic scintillator elements arranged in a cylinder of mean radius of about 81 cm, which is mounted on the outer surface of the carbon fiber composite shell of the MDC. The two single layer end caps, each with 48 trapezoidal shaped scintillation counters, are located outside the MDC end caps. The scintillator is 5 cm thick and 48 cm long. Each counter is read out from one end of the scintillator by a single fine mesh PMT. The solid angle coverage of the barrel TOF is $|\cos\theta| < 0.83$, while that of the end cap is $0.85 < |\cos\theta| < 0.95$. TOF counters also play a critical role as fast triggers for charged particles.
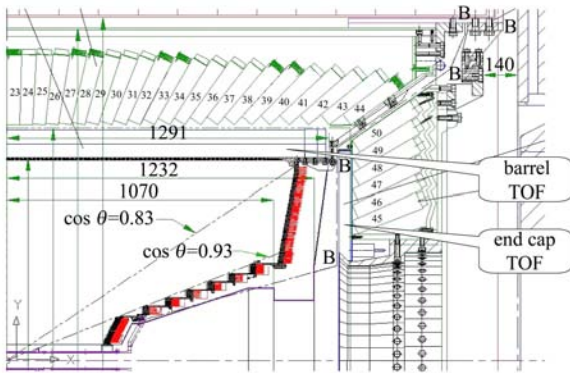
Fig. 1.   Schematic drawing of the TOF on BESIII.

3   Time calibration for the end cap TOF

3.1   TOF raw data

In the case of beam collision events, BEPC II will be operated in the two-ring and multi-bunch colliding mode, and 93 bunches with the bunch spacing of 8 ns will be filled in each storage ring. The time measurement system of the TOF adopts CERN HPTDC (High Performance Time to Digital Converter) chip. The trigger cycle is 24 ns, which equals the duration of 3 bunches. When two bunches collide and generate a good event, the raw measured time TDC recorded by electronics is the time interval of the start time to the arrival time of the detector's hit signal. This time interval may differ from that between the collision and the arrival time of the hit signal in the detector. The interval of the trigger start time to the real collision time is described as the event start time t_0 [4]. The measured time of flight from the collision to the arrival time is expressed as t_{raw},

$$t_{\text{raw}} = \text{TDC} - t_0. \tag{1}$$

The pulse height(charge) of the hit signal is proportional to the time interval from the charge to time conversion(QTC) output which is measured by HPTDC [5]. Fig. 2(a) and (b) show the raw measured time t_{raw} and corresponding pulse height distributions, respectively. The electrons in Bhabha events are used for these plots.
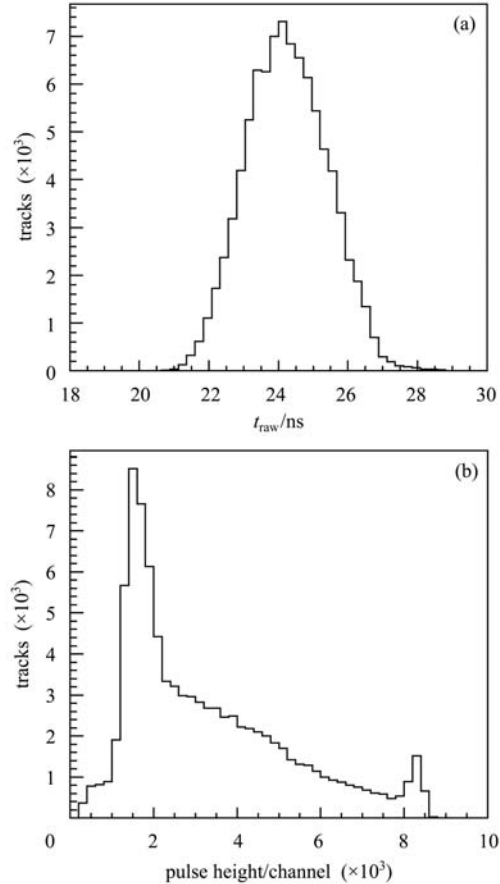
Fig. 2.   Distributions of the raw measured time (a) and pulse height (b) of electrons in Bhabha events.

3.2   The pulse height correction

There is an obvious bump near the 8200 channel in the distribution of pulse height shown in Fig. 2(b), which is caused by the electronics saturation. The pulse height distribution is adequately described by the highly-skewed Landau distribution for plastic scintillator bars [6]. The long Landau "tail" extends beyond the dynamic range of the TOF electronics readout system.

The amplitude-dependence time-walk correction, which is an important part of time calibration for the TOF, should be accomplished by measuring the corresponding pulse height. The electronics scan curve of each channel is obtained to make the pulse height

correction in order to reduce the impact of the electronics saturation on the time resolution. The following smooth function,

$$f(x) = a_0 + a_1 \cdot x + a_2 \cdot x^2 + a_3 \cdot x^3 + a_4 \cdot x^4$$

$$+ a_5 \cdot \exp\left(\frac{x - a_6}{a_7}\right), \tag{2}$$

is used to fit, $a_0 - a_7$ are the fit parameters. The hit position along the direction of the scintillator (z for barrel and r for end cap) of each track is reconstructed using the MDC track trajectory extrapolation [7]. A typical electronics scan curve is shown in Fig. 3(a), (b) shows the corrected pulse height distribution using electronics scan curve of the electrons, (c) and (d) are the scattering plots of the pulse height versus the r hit position before and after the pulse height correction, respectively.
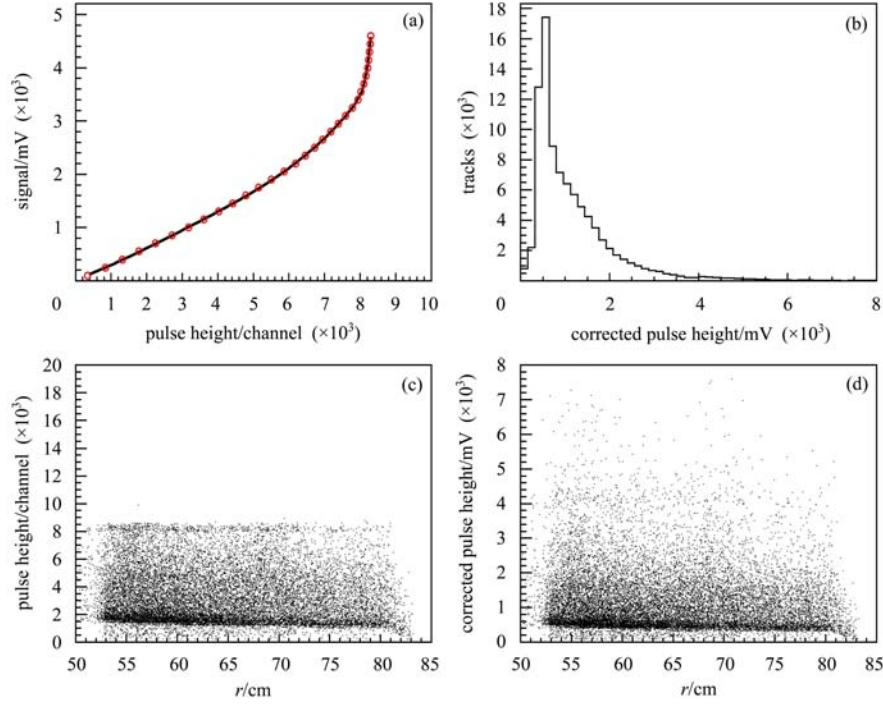
Fig. 3. (a) A typical electronics scan curve. (b) The corrected pulse height using an electronics scan curve. (c) The scattering plot of pulse height versus r hit position. (d) The scattering plot of corrected pulse height versus r hit position.

3.3 The predicted time

A track fitting algorithm based on the Kalman filter method has been employed for MDC reconstruction [8]. The Kalman filter method updates the fitting results in each step with the addition of measurement points, then it deals with multiple scattering, energy loss and non-uniformity of magnetic field as a deviation with a Gaussian distribution in each step, to yield more accurate track parameters and an error matrix. The accurate predicted time t_{pred} calculated using the Kalman filter method is expressed as

$$t_{\mathrm{pred}}^{\mathrm{i}} = \sum_{\mathrm{step}} t_{\mathrm{step}}^{\mathrm{i}} + t_{\mathrm{TOF}}^{\mathrm{i}}, \tag{3}$$

where the first item is the time of flight from the interaction point to the outer wall of the MDC, and the second item is from the outer wall to the scintillator.

In general, the $t_{\mathrm{step}}^{\mathrm{i}}$ is the predicted time of each step in the MDC,

$$t_{\mathrm{step}}^{\mathrm{i}} = \frac{L_{\mathrm{step}}}{\beta_{\mathrm{step}}^{\mathrm{i}} \cdot c}, \tag{4}$$

where i is the desired particle hypothesis (e, μ, π, K, p), L_{step} is the corresponding path of flight of this step, c is the velocity of light in a vacuum, the flight velocity of the charged particle in this step $\beta_{\mathrm{step}}^{\mathrm{i}} = p/\sqrt{p^2 + m_{\mathrm{i}}^2}$, p is the measured momentum using the Kalman filter algorithm in this step and m_{i} is the mass of the particle i. The predicted time outside the MDC could be calculated using a similar formula. The predicted time obtained using the Kalman filter method is more accurate than the one calculated with the assumption that the track trajectory moving in the detector is described as a standard helix.

3.4 The time calibration

The calibration of the TOF is carried out by comparing the measured time $t_{\mathrm{mea}} = t_{\mathrm{raw}} - t_{\mathrm{cor}}$ against the predicted time t_{pred},

$$\Delta t = t_{\mathrm{mea}} - t_{\mathrm{pred}}, \tag{5}$$

where t_{cor} is the correction term. The correction term t_{cor} is a function of the pulse height Q and the hit position r. For the end cap TOF, we take the following 7-term empirical form,

$$t_{\mathrm{cor}} = P_0 + \frac{P_1}{\sqrt{Q}} + \frac{P_2}{Q} + P_3 \cdot Q + P_4 \cdot r + P_5 \cdot r^2$$
$$+ P_6 \cdot r^3, \tag{6}$$

where $P_i (i=0,1,...,6)$ are the calibration constants: P_0 represents the delay time, such as cabling, etc.; the correction function of the time walk effect is represented by the term containing P_1; P_2 and P_3 are used to describe the saturation of the electronics, etc.; and a polynomial containing P_4 and P_6 describes the correction to the effective velocity of light in the scintillator.

A χ^2 minimization method is applied by defining a set of

$$\chi^2(\text{readout unit}) = \sum^{\text{event}} (t_{\mathrm{mea}} - t_{\mathrm{pred}})^2 \tag{7}$$

in each readout unit independently. The calibration constants, P_0 to P_6, are obtained from offline data, electrons in Bhabha events or muons in dimu events,

by setting the derivative of Eq. (7) with respect to P_i to zero.

3.5 Calibration sample

Electrons in Bhabha events and muons in dimu events are both data sample candidates for time calibration for the end cap TOF. The scattering plots of raw measured time t_{raw} versus the r hit position of electrons and muons are shown in Fig. 4(a) and (b), respectively. For each specific r region, the distribution of raw measured time of electrons is wider than that of muons. There are some materials, such as cables and electronics equipment, between the endplate of the outer chamber of MDC and the end cap TOF. The muons in dimu events do not have large electromagnetic showers or hadronic interactions, while material interactions of electrons in Bhabha events generate showers which are recorded by the TOF electronics as fake signals. Two Monte Carlo samples of Bhabha events are generated with and without simulation of the materials between the MDC and the TOF. The raw measured time versus the r hit position scattering plots are shown in Fig. 4(c) and (d), respectively. It could be found that the scattering plot of t_{raw} versus r of the MC sample of electrons without simulation of materials is similar to that of the real muon data. For electrons in Bhabha events, another shortage is that electrons are frequently accompanied by backsplash from the CsI calorimeter behind the TOF counters.
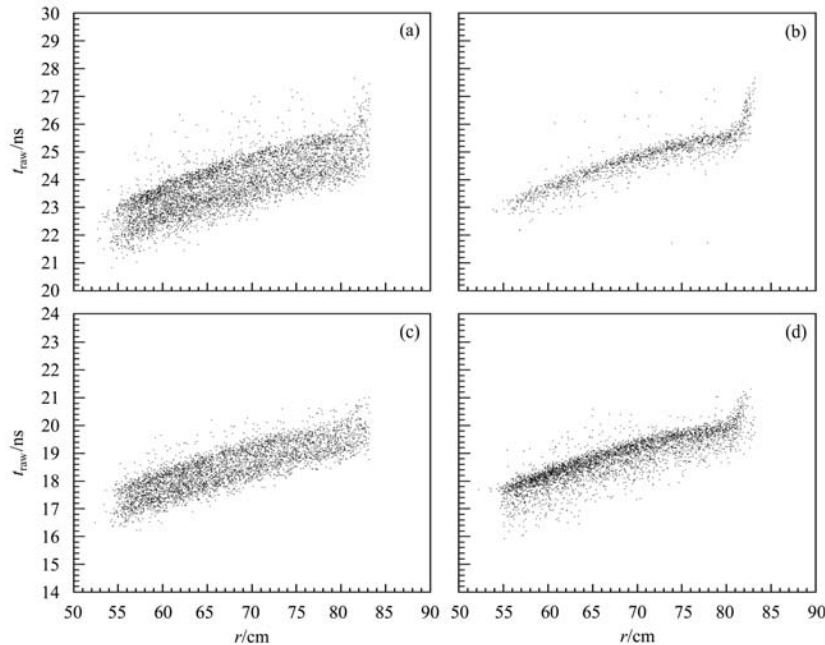
Fig. 4. The scattering plots of raw measured time vs the r hit position of electrons in Bhabha events (a) and muons in dimu events; (b) the scattering plots of raw measured time vs the r hit position of the MC sample of electrons with (c) and without (d) simulation of materials between the MDC and the TOF.

The time resolution is related to many items, such as the intrinsic time resolution of the scintillator, the uncertainty from bunch length and bunch time, the uncertainty from extrapolated hit position, the uncertainty from electronics, the resolution of predicted time of flight and time walk effect, and so on [2]. In these factors affecting the time resolution, the bunch length and the bunch time are strongly associated with the status of the accelerator. Frequent calibration of the TOF is necessary in order to minimize the effect of these uncertainties. In the τ-c energy region, the cross section of Bhabha is much higher than that of dimu. Compared with the muons, the electrons more easily satisfy the statistic requirement for frequent calibration.

3.6   Time difference versus pulse height

We have investigated the applications of the calibration constants obtained from electrons and muons, respectively. The control sample is π mesons from the decay channel $J/\psi \to \rho\pi$. The scattering plots of time differences Δt defined as Eq. (6) versus the corrected pulse height with applications of two different calibration samples are shown in Fig. 5 (a) and (b), respectively.

The Δt offset is obvious with a high corrected pulse height value using calibration constants obtained from muons compared with electrons. The corrected pulse height distributions of pions and muons are shown in Fig. 5(c) and (d), respectively. The statistic of muons with high pulse height value is limited and its pulse height does not cover the saturation range. The time correction of the high pulse height using calibration constants obtained from muons is the extension of the experience of the low pulse height value. Although the time resolution of pions using calibration constants obtained from muons is slightly better, big offsets are also introduced for particles with a high pulse height value at the same time.
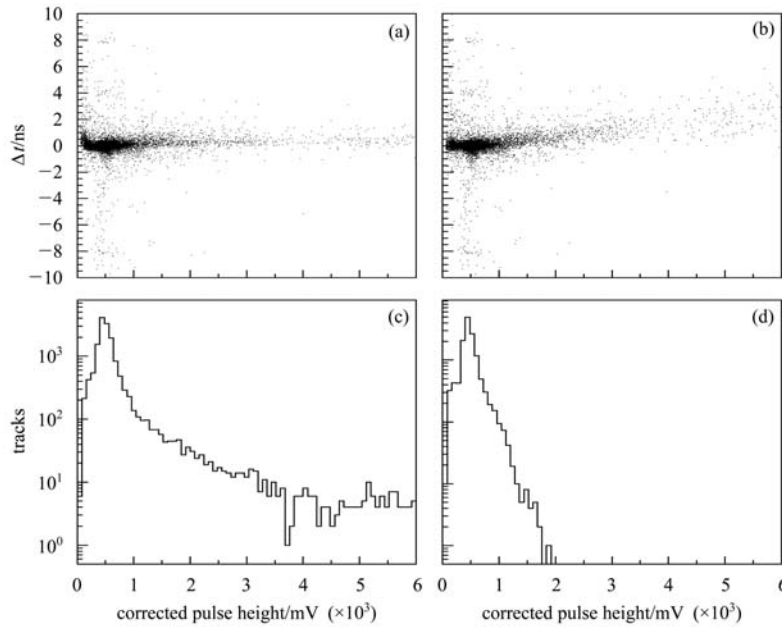
Fig. 5.   The scattering plots of time difference versus the corrected pulse height of pions using calibration constants obtained from electrons in Bhabha events (a) and muons in dimu events (b); the corrected pulse height distributions of pions (c) and muons (d).

4   Results of time calibration and performance check

By applying the 7-term empirical function Eq. (6), the results of time calibration are obtained using electrons in Bhabha events and muons in dimu events as a calibration sample, respectively. Fig. 6(a) and (b) show the time resolution improved from 747 ps to 148 ps with the correction of time of flight for elec-

trons. (c) and (d) show the time resolutions before and after the calibration for muons, which are 563 ps and 110 ps, respectively. Although the time resolution of muons is better than that of electrons caused by the endplate material interaction, the electrons in Bhabha events are chosen as a calibration sample which are satisfied for frequent calibration and supported by the results of performance check for hadrons.

The control samples of pions and kaons are used to apply the performance check of capability of K/π separation using calibration constants obtained from electrons in Bhabha events. The pions are chosen from decay channel $J/\psi \rightarrow \rho\pi$ and kaons are from $J/\psi \rightarrow K^{\pm}K^*(892)^{\mp}$ with $K^*(892)^{\mp} \rightarrow K^{\mp}\pi^0$. The flight time difference of kaon and pion with the same momentum, $\Delta t_{K/\pi} = t^K_{pred} - t^\pi_{pred}$, and the time resolu-

tion $\sigma_{K/\pi}$ could be obtained from the control sample. A 2σ separation corresponds to $\Delta t_{K/\pi} > 3.38\sigma_{K/\pi}$, where $\sigma_{K/\pi}$ is the time resolution with an assumption that the time difference is a standard Gaussian distribution. Fig. 7(a) and (b) show the time resolutions for pions and kaons at 1.0 GeV respectively, (c) shows the capability of K/π separation, and the transverse axis is the polar angle.
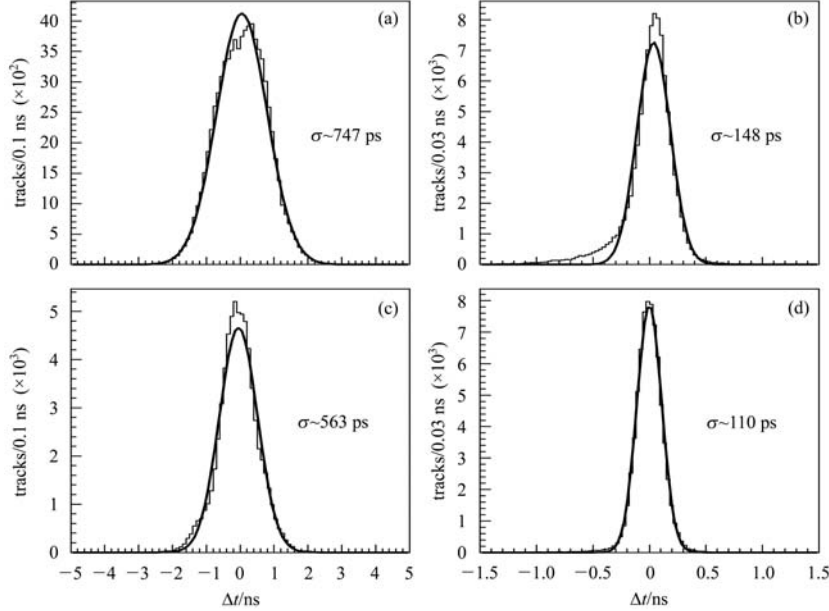
Fig. 6. Δt distributions: before (a) and after (b) calibration for electrons; before (c) and after (d) calibration for muons.
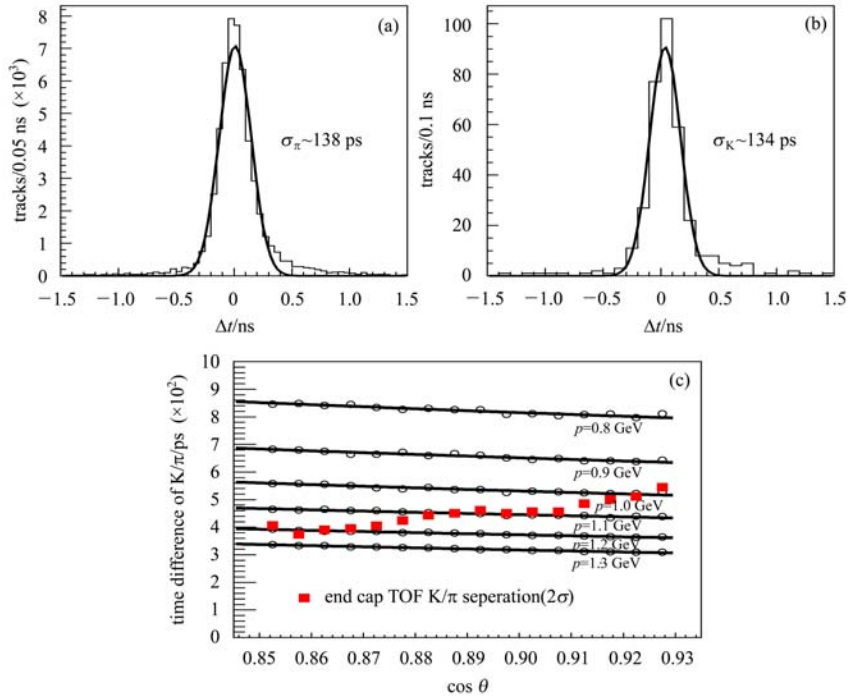
Fig. 7. Δt distributions for pions (a) and kaons (b) at 1.0 GeV. (c) Capability of kaon and pion separation.

5   Discussion and summary

The capability of particle identification by the TOF detector requires a good time resolution. In this paper, the calibration for the end cap TOF of BESIII is presented. It has achieved about 110 ps time resolution for muons in dimu events, which reaches the designed goal of 110 ps [2]. This time resolution is obtained using the whole J/ψ data, which reflect the general status of BESIII and BEPCII, not only the high quality data sample, although its time resolution is better than this value. The electronics scan curve of each electronics channel is obtained to correct the measured pulse height values which are beyond the dynamic range. The Kalman filter method is employed to calculate the predicted time step by step, instead of taking the track trajectory as a standard helix. The material interactions of electrons in Bhabha events would generate showers as fake signals recorded by TOF electronics, which cause the asymmetry of Δt distribution and worse time resolution compared with muons. The preliminary performance check of hadron samples shows the existence of big offsets of time difference with high pulse height values applying the calibration constants obtained using muons in dimu events since muons cover a relatively short pulse height range. Further possible improvement is expected from more accurate electronics scan curves. The capability of K/π separation of the end cap TOF is also described in this paper.

References

1 ZHANG C for BEPC & BEPCII Teams. Performance of the BEPC and progress of the BEPCII. In: Proceedings of APAC, Gyeongju Korea, 2004, 15–19
2 BESIII collaboration. The Preliminary Design Report of the BESIII Detector. Beijing: IHEP-BEPCII-SB-13, 2004
3 Ablikim M et al. Nuclear Instruments and Methods in Physics Research A, 2010, **614**: 345–399
4 MA Xiang, MAO Ze-Pu et al. HEP & NP, 2008, **32**(9): 744–749
5 LIU Shu-Bin, FENG Chang-Qing, AN Qi et al. IEEE Transactions on Nulcear Science, 2010, **57**(2)**:** 419–427
6 Particle Data Group. Phys. Lett. B, 2008, **667**
7 WANG Liang-Liang, YUAN Chang-Zheng et al. HEP & NP, 2007, **31**(2): 183–188 (in Chinese)
8 WANG Ji-Ke, MAO Ze-Pu, et al. Chinese Physics C (HEP & NP), 2009, **33**(10): 870–879